



## Orchestrating in the Sky: Joint Routing and Client Selection for Federated Learning in LEO Networks

Zhao, Yi; Yu, Zhanwei; Feng, Chenyuan; You, Lei; Lei, Lei; Yuan, Di

*Published in:*  
Proceedings of IEEE GLOBECOM 2025

*Link to article, DOI:*  
[10.1109/GLOBECOM59602.2025.11432690](https://doi.org/10.1109/GLOBECOM59602.2025.11432690)

*Publication date:*  
2026

*Document Version*  
Peer reviewed version

[Link back to DTU Orbit](#)

*Citation (APA):*  
Zhao, Y., Yu, Z., Feng, C., You, L., Lei, L., & Yuan, D. (2026). Orchestrating in the Sky: Joint Routing and Client Selection for Federated Learning in LEO Networks. In *Proceedings of IEEE GLOBECOM 2025 IEEE*.  
<https://doi.org/10.1109/GLOBECOM59602.2025.11432690>

---

### General rights

Copyright and moral rights for the publications made accessible in the public portal are retained by the authors and/or other copyright owners and it is a condition of accessing publications that users recognise and abide by the legal requirements associated with these rights.

- Users may download and print one copy of any publication from the public portal for the purpose of private study or research.
- You may not further distribute the material or use it for any profit-making activity or commercial gain
- You may freely distribute the URL identifying the publication in the public portal

If you believe that this document breaches copyright please contact us providing details, and we will remove access to the work immediately and investigate your claim.

# Orchestrating in the Sky: Joint Routing and Client Selection for Federated Learning in LEO Networks

Yi Zhao<sup>1</sup>, Zhanwei Yu<sup>1</sup>, Chenyuan Feng<sup>2</sup>, Lei You<sup>3</sup>, Lei Lei<sup>4</sup>, and Di Yuan<sup>1</sup>

<sup>1</sup>Department of Information Technology, Uppsala University, 75105 Uppsala, Sweden.

<sup>2</sup>College of Computer Science, University of Exeter, EX4 4QJ Devon, UK.

<sup>3</sup>Department of Engineering Technology, Technical University of Denmark, 2750 Ballerup, Denmark.

<sup>4</sup>School of Information and Communications Engineering, Xi'an Jiaotong University, 710049 Xi'an, China.

Emails: {yi.zhao; zhanwei.yu; di.yuan}@it.uu.se, c.feng@exeter.ac.uk, leiyo@dtu.dk, lei.lei@xjtu.edu.cn

**Abstract**—Federated Learning (FL) on low earth orbit (LEO) satellites represents a promising frontier for on-orbit edge intelligence. However, the inherent network dynamics and heterogeneity of datasets and resource across satellites pose challenges to efficient on-orbit FL. In this work, we model client selection and inter-satellite routing as a joint optimization problem. We derive and minimize an upper bound of the global empirical loss as the objective function, to enable fast convergence. We model the constraints of inter-satellite routing via time-varying graphs and network flow theory. We propose both exact and approximate solutions for the joint optimization problem. In addition, we formalize and prove the convergence property of our approach. Last, by simulation we demonstrate the efficiency and superiority of the proposed scheme for realistic satellite networking scenarios.

**Index Terms**—Satellite networks, federated learning, client selection, inter-satellite routing, time-varying graphs.

## I. INTRODUCTION

Federated Learning (FL) [1] is a paradigm for distributed machine learning among collaborative devices. In FL, multiple clients train a model using their local datasets, and then send locally updated model parameters to a server for global aggregation. Deploying FL on low earth orbit (LEO) satellites is promising in enabling real-time on-orbit edge intelligence for tasks such as remote sensing and target tracing [2]. Compared with the traditional FL on ground, or FL on satellites with the ground station as the server [3], FL that operates entirely at the edge of space [4]–[6], i.e., both the server and clients are LEO satellites, avoids the bottleneck of satellite-ground links' limited bandwidth and connection time. In this scenario, the dynamic topology poses challenge to satellites' collaboration.

Client selection [7], [8], that is to determine which clients participate in each round of training, plays a critical role in the efficiency of FL. Involving as many clients as possible causes the diminishing effect and slows down the convergence [1]. Besides, not all devices contribute to the global model with high-quality updates, as they differ in the quality and distribution of local data, and communication and computing resource. What has been proposed is to let a fixed fraction of devices participate in each round [1], and they can be selected randomly (i.e., unbiased selection), or with bias toward the devices contributing the most to the convergence. Common

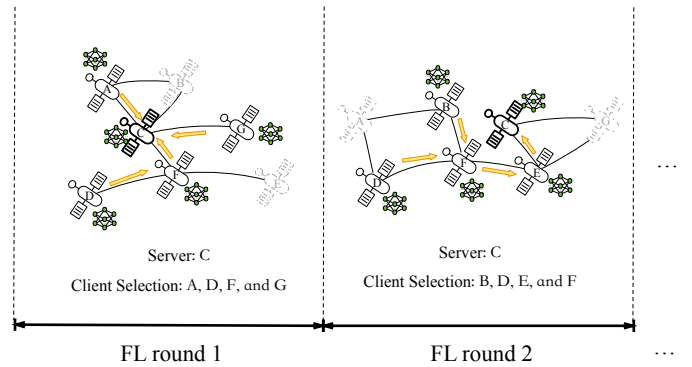


Figure 1: Client selection and inter-satellite routing for FL over satellite networks.

metrics for client selection include data utility (e.g., dataset size and distribution), model utility (e.g., loss and gradient norm), and system utility (e.g., computational frequency, memory, battery, and channel). Besides the heterogeneity of data and constrained resources, one additional challenge of FL in the on-orbit context is that the client selection is not device-independent, but mutually coupled and constrained to routing on dynamic network topology, as illustrated in Fig. 1.

For on-orbit FL, the study in [4] investigated the server selection and resource allocation problem. The research in [5] proposed a decentralized framework and a threshold-based and iterative offloading algorithm. The authors of [6] optimized the number of orbits and the number of satellites per orbit to minimize the convergence time. For client selection in FL, we refer to surveys [7] and [8]. To summarize, the existing algorithms can be classified into metric-based methods and mechanism-based methods, such as clustering, optimization, and machine learning. In particular, the study in [9] designed a strategy based on the norms of local gradients. The research in [10] presented the convergence analysis of FL with general biased client selection, and designed an algorithm based on local loss. The authors of [11] modeled an optimization problem to minimize the accuracy loss and cost of FL, and proposed an algorithm based on problem decomposition.

To the best of our knowledge, this is the first paper that

jointly optimizes the client selection and routing for FL on satellite networks. For this problem, our contributions are as follows: 1) We derive and minimize an upper bound of the global empirical loss as the objective function, to enable fast convergence. 2) We model the constraints of inter-satellite routing via time-varying graphs [12], [13] and network flow theory. 3) We propose both exact and approximate solutions for the joint optimization problem, and provide the theoretical convergence analysis. 4) We show simulation results to demonstrate the efficiency and superiority of the proposed scheme for realistic satellite networking scenarios.

## II. SYSTEM MODEL

### A. Federated Learning

One satellite is designated as the server that stores the predicted periodical network topologies. At the beginning of each round of FL, the server sends global model parameters to the satellites in a candidate client set. These satellites train the received model locally using their datasets, and return the respective metric values. Next, the server selects the clients according to the feedback and the routing constraints, followed by informing the selected clients to return their local parameter updates, and making the global aggregation.

Denote by  $\mathcal{I} = \{1, 2, \dots, I\}$  the set of satellites in a given LEO constellation for FL. Denote by  $\mathcal{T} = \{1, 2, \dots, T\}$  the set of rounds of FL. The duration of each round is given. Note that the network topology within one round may change. We have binary variable  $\theta$  and  $x$  to indicate the candidate set and client selection, respectively. Variable  $\theta_t^i = 1$  if satellite  $i$  is within the candidate set of clients in round  $t$  of FL; otherwise  $\theta_t^i = 0$ . Variable  $x_t^i = 1$  if satellite  $i$  is selected as a client in round  $t$  of FL; otherwise  $x_t^i = 0$ .

For each round  $t$ , a satellite can be selected as a client only if it is in the candidate set. Hence we have:

$$x_t^i \leq \theta_t^i, \quad i \in \mathcal{I}. \quad (1)$$

We adopt the FedAvg algorithm [1] for FL, which has a fixed fraction  $C \in [0, 1]$  of devices as clients in each round  $t$ , such that  $IC$  is an integer, hence we have:

$$\sum_{i \in \mathcal{I}} x_t^i = IC. \quad (2)$$

Denote by  $w_t$  and  $w_t^i$  respectively the global model parameters at the server, and the local model parameters on satellite  $i$ , by the end of round  $t$ . Consider the stochastic gradient descent (SGD) method with learning rate  $\eta$ . There are two updates of model parameters:

1) *Local Training*: In round  $t$ , each satellite  $i$  in the candidate set receives model parameters  $w_{t-1}$  from the server, and trains the model according to its local dataset with  $N_t^i$  samples. The local model is updated as follows:

$$w_t^i = w_{t-1} - \eta \theta_t^i \nabla f_i(w_{t-1}), \quad (3)$$

where  $f_i(\cdot)$  is the local loss function on a random batch of data samples on satellite  $i$ , and  $\nabla f_i(\cdot)$  is its gradient.

2) *Global Aggregation*: The server collects the updates of model parameters from selected clients, and takes the weighted average, formulated below:

$$w_t = \sum_{i \in \mathcal{I}} \gamma_t^i x_t^i w_t^i = w_{t-1} - \eta \sum_{i \in \mathcal{I}} \gamma_t^i x_t^i \nabla f_i(w_{t-1}), \quad (4)$$

where  $\gamma_t^i$  is the weight of satellite  $i$ ; it is set according to the normalized size of its local dataset, i.e.,  $\gamma_t^i = \frac{N_t^i}{\sum_{i \in \mathcal{I}} N_t^i}$ , and  $\sum_{i \in \mathcal{I}} \gamma_t^i = 1$ .

### B. Inter-Satellite Routing Model

During a round of FL, the network topology may change, hence we consider time-varying graphs [12] to model the dynamics. Compared with static and pre-calculated routing, routing based on time-varying graphs is more effective, flexible, and robust for satellite networks [14]. A time-varying graph consists of a sequence of inter-connected static network topologies. Each of them corresponds to a so-called snapshot [13]. There are two types of links:

1) *Intra-snapshot link*: The presence of a link between two satellites within a snapshot means a single-hop communication connectivity, which is symmetric (we use the term arc to refer to either direction). The capacity of an intra-snapshot arc represents the maximum possible data volume of communication through this arc over the duration of the snapshot, normalized with respect to the model size (i.e., the floor of the product of snapshot duration and link rate divided by the model size).

2) *Inter-snapshot link*: Such a link only exists for two nodes corresponding to the same satellite in two consecutive snapshots. It is used to model local caching along time. We assume that the cache capacity is not a limiting factor, and therefore set the capacity of any inter-snapshot link to be  $I$ .

Denote by  $s$  the index of the server satellite. Denote by  $G_t = (V_t, E_t)$  the time-varying graph of satellites in round  $t$ , where  $V_t$  and  $E_t$  are the sets of vertexes and arcs respectively. Denote by  $\mathcal{K}_t = \{1, 2, \dots, K_t\}$  the set of snapshots of round  $t$  for the routing problem<sup>1</sup>. Both  $G_t$  and  $\mathcal{K}_t$  can be pre-calculated, as the duration of round  $t$  is given, and the satellites operate in their orbits periodically. Denote by  $h_t^k$  the duration from the beginning of round  $t$  to the end of its  $k$ th snapshot. To distinguish between the same satellite in different snapshots in mathematical modeling, we use  $i \setminus k$  as a shorthand notation for tuple  $(i, k)$ , to refer to the graph node of satellite  $i$  in snapshot  $k$ . Denote by  $c^{(u,v)}$  the capacity of arc  $(u, v) \in E_t$ . We have two model parameter transmissions within  $\mathcal{K}_t$ : Model downloading from the server to candidate clients, and model uploading from the selected clients to the server<sup>2</sup>.

1) *Downloading*: Variable  $y_t^{ik} = 1$  if satellite  $i$  finishes its downloading by the end of snapshot  $k$  in round  $t$ ; otherwise

<sup>1</sup>The averaging operation and global parameter updates on the server are not related to network topology, and it takes place at the end of each round  $t$ , hence we assume enough time is reserved after snapshot  $K_t$  for this purpose.

<sup>2</sup>The time of metric aggregation and informing selected clients is short, and hence omitted in modeling.

$y_t^{ik} = 0$ . Variable  $y_t^{ik}$  can be one only if satellite  $i$  is in the candidate set in round  $t$ , hence we have:

$$\sum_{k \in \mathcal{K}_t} y_t^{ik} = \theta_t^i, \quad i \in \mathcal{I}. \quad (5)$$

Denote by  $\phi_t^{\downarrow(u,v)}$  the downloading flow on arc  $(u,v) \in E_t$ , i.e., the number of times that the global model is transmitted (for different candidate clients) via  $(u,v)$  in round  $t$ . Note that multiple copies of the global model parameters are transmitted in the network simultaneously. Since  $\phi_t^{\downarrow(u,v)}$  does not carry information of destination, flow arriving at a satellite is not distinguishable with respect to which part of the global model it contains. That is, fractional flows entering a candidate client, even though summing up to one, do not guarantee the recipient of the whole global model as they may contain overlapping parts. Therefore  $\phi_t^{\downarrow(u,v)}$  is restricted to be integer. We have link capacity constraint  $\phi_t^{\downarrow(u,v)} \leq c^{(u,v)}$ ,  $(u,v) \in E_t$ , and the flow balance constraints for downloading of node  $i \setminus k$ :

$$\sum_{(ik,v) \in E_t} \phi_t^{\downarrow(ik,v)} - \sum_{(v,ik) \in E_t} \phi_t^{\downarrow(v,ik)} = \begin{cases} CI, & i = s, k = 0 \\ -y_t^{ik}, & \text{otherwise} \end{cases} \quad i \in \mathcal{I}, k \in \mathcal{K}_t. \quad (6)$$

2) *Uploading*: Variable  $z_t^{ik} = 1$  if satellite  $i$  starts its uploading at the beginning of snapshot  $k$  in round  $t$ ; otherwise  $z_t^{ik} = 0$ . Thus we have:

$$\sum_{k \in \mathcal{K}_t} z_t^{ik} = x_t^i, \quad i \in \mathcal{I}. \quad (7)$$

Denote by  $\phi_t^{\uparrow(u,v)}$  the uploading flow on arc  $(u,v) \in E_t$ . Different from downloading, a single copy of the model parameters of each selected client is uploaded. Hence the model parameters originating from a client can be delivered to the server via multiple paths, i.e.,  $\phi_t^{\uparrow(u,v)}$  is allowed to be fractional. Considering the flow going through node  $i \setminus k$ , we have the flow balance constraints below:

$$\sum_{(ik,v) \in E_t} \phi_t^{\uparrow(ik,v)} - \sum_{(v,ik) \in E_t} \phi_t^{\uparrow(v,ik)} = \begin{cases} -CI, & i = s, k = K_t \\ z_t^{ik}, & \text{otherwise} \end{cases} \quad i \in \mathcal{I}, k \in \mathcal{K}_t \quad (8)$$

and the link capacity constraint  $\phi_t^{\uparrow(u,v)} \leq c^{(u,v)}$ ,  $(u,v) \in E_t$ .

In addition, parameter  $H_t^i$  denotes the time reserved for local training<sup>3</sup> of satellite  $i$  in round  $t$ . We then have:

$$\sum_{k \in \mathcal{K}_t} h_t^{k-1} z_t^{ik} - \sum_{k \in \mathcal{K}_t} h_t^k y_t^{ik} \geq x_t^i H_t^i - (1 - x_t^i) \sum_{k \in \mathcal{K}_t} h_t^k, \quad i \in \mathcal{I}. \quad (9)$$

An example of routing on time-varying graph is given in Fig. 2.

<sup>3</sup>The energy supply and other computational loads of a satellite may change along time, and we assume that each satellite reports its availability for FL and the required time for local training before the beginning of each round. The satellites that fail to report this information due to communication unreachability are excluded for the current round of FL.

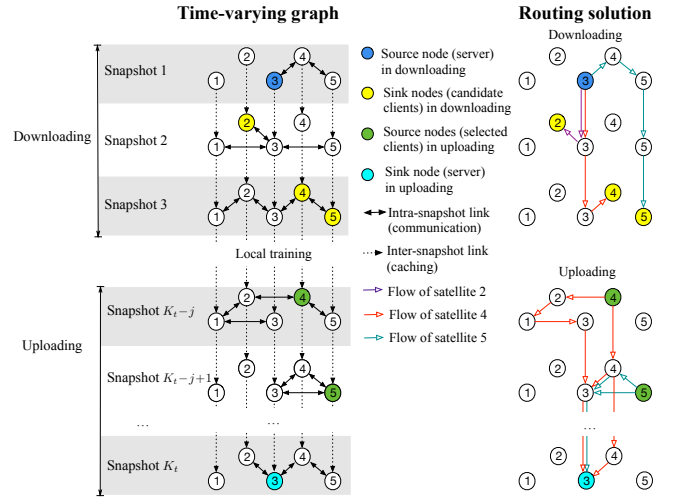


Figure 2: An example of time-varying graph of satellite network, and the routing for downloading and uploading.

### C. Problem Formulation

The global empirical risk [10] in a round of FL is the weighted average of local loss over all selected clients. Denote the global empirical risk by  $F(\mathbf{w}_t)$  for round  $t$ , we have:

$$F(\mathbf{w}_t) = \sum_{i \in \mathcal{I}} \gamma_t^i x_t^i f_i(\mathbf{w}_t). \quad (10)$$

The global expected risk is  $\mathbb{E}\{F(\mathbf{w}_t)\}$  where the expectation is over the distribution of random data samples for local training. This function is, however, empirical, implicit, and non-linear in the client selection variables. For tractability, we consider an upper bound of the global expected risk, denoted by  $U(\cdot)$ . The joint client selection and dynamic routing problem of FL is then formulated below.

$$\min_{\theta, \mathbf{x}, \mathbf{y}, \mathbf{z} \text{ binary}, \phi^{\downarrow} \in \text{integer}, 0 \leq \phi^{\downarrow} \leq c, 0 \leq \phi^{\uparrow} \leq c} U(\mathbb{E}\{F(\mathbf{w}_t)\}) \quad (11a)$$

s.t. (1) and (2) for client selection

(6) and (8) for routing

(5), (7), and (9) for variable coupling

## III. ALGORITHM

### A. Upper Bound of Empirical Risk

**Basic Assumptions** (the last two are necessary only for the convergence analysis in Section III-C):

- The global empirical risk function  $F(\mathbf{w}_t)$  is L-smooth:  $\|\nabla F(\mathbf{w}_i) - \nabla F(\mathbf{w}_j)\| \leq L\|\mathbf{w}_i - \mathbf{w}_j\|, \forall \mathbf{w}_i, \mathbf{w}_j$ .
- Divergences of global and local empirical risk functions are bounded:  $\|\nabla F(\mathbf{w}_t) - \nabla f_i(\mathbf{w}_t)\|^2 \leq \epsilon^2, \forall \mathbf{w}_t, i \in \mathcal{I}$ .
- The global empirical risk function  $F(\mathbf{w}_t)$  is lower-bounded:  $F(\mathbf{w}_t) \geq F_{\text{inf}}, \forall \mathbf{w}_t$ .
- The sum weight of selected clients in each round is lower-bounded:  $\sum_{i \in \mathcal{I}} x_t^i \gamma_t^i \geq A_{\text{lb}}, \forall t \in \mathcal{T}$ .

**Theorem 1.** *The following function in  $\mathbf{x}$  is a valid upper bound of  $F(\mathbf{w}_t)$ :*

$$U(F(\mathbf{w}_t)) = \mathbb{E}\{F(\mathbf{w}_{t-1})\} + \frac{\eta}{2} \sum_{i \in \mathcal{I}} x_t^i \gamma_t^i \{(LCI\eta\gamma_t^i - 1) \times \mathbb{E}\{\|\nabla f_i(\mathbf{w}_{t-1})\|^2\} + \epsilon^2 - \mathbb{E}\{\|\nabla F(\mathbf{w}_{t-1})\|^2\}\}. \quad (12)$$

*Proof.*

$$\mathbb{E}\{F(\mathbf{w}_t)\} = \mathbb{E}\left\{F\left(\mathbf{w}_{t-1} - \eta \sum_{i \in \mathcal{I}} \gamma_t^i x_t^i \nabla f_i(\mathbf{w}_{t-1})\right)\right\} \quad (13a)$$

$$\leq \mathbb{E}\{F(\mathbf{w}_{t-1})\} + \frac{L\eta^2}{2} \mathbb{E}\left\{\left\|\sum_{i \in \mathcal{I}} \gamma_t^i x_t^i \nabla f_i(\mathbf{w}_{t-1})\right\|^2\right\} - \eta \mathbb{E}\left\{\left\langle \nabla F(\mathbf{w}_{t-1}), \sum_{i \in \mathcal{I}} \gamma_t^i x_t^i \nabla f_i(\mathbf{w}_{t-1}) \right\rangle\right\} \quad (13b)$$

where (13a) holds by substitution of  $\mathbf{w}_t$  by (4), and (13b) holds due to the smoothness of  $F(\cdot)$  such that  $F(\mathbf{a}) \leq F(\mathbf{b}) + \frac{L}{2}\|\mathbf{a} - \mathbf{b}\|^2 + \langle \nabla F(\mathbf{b}), \mathbf{a} - \mathbf{b} \rangle$  for any two vectors  $\mathbf{a}$  and  $\mathbf{b}$  of same size.

Denote by  $\text{RHS}_{(13b)}^2$  and  $\text{RHS}_{(13b)}^3$  the second and third terms of (13b), respectively. We have:

$$\text{RHS}_{(13b)}^2 \leq \frac{LCI\eta^2}{2} \sum_{i \in \mathcal{I}} \mathbb{E}\left\{\left\|\gamma_t^i x_t^i \nabla f_i(\mathbf{w}_{t-1})\right\|^2\right\} \quad (14a)$$

$$= \frac{LCI\eta^2}{2} \sum_{i \in \mathcal{I}} (\gamma_t^i)^2 x_t^i \mathbb{E}\{\|\nabla f_i(\mathbf{w}_{t-1})\|^2\} \quad (14b)$$

where (14a) holds because of Jensen's inequality that  $\|\sum_{i=1}^M b_i\|^2 \leq M \sum_{i=1}^M \|b_i\|^2$  for any integer  $M \geq 1$  and vector  $\mathbf{b}$ . And (14b) holds due to that  $\mathbb{E}\{\|m\mathbf{b}\|^2\} = m^2 \mathbb{E}\{\|\mathbf{b}\|^2\}$  for any  $m$  and  $\mathbf{b}$ , and  $x_t^i$  is binary so that  $(x_t^i)^2 = x_t^i, i \in \mathcal{I}, t \in \mathcal{T}$ .

For the third term in (13b), we have:

$$\text{RHS}_{(13b)}^3 = -\eta \sum_{i \in \mathcal{I}} \gamma_t^i x_t^i \mathbb{E}\{\langle \nabla F(\mathbf{w}_{t-1}), \nabla f_i(\mathbf{w}_{t-1}) \rangle\} \quad (15a)$$

$$= \frac{\eta}{2} \sum_{i \in \mathcal{I}} \gamma_t^i x_t^i \mathbb{E}\{\|\nabla F(\mathbf{w}_{t-1}) - \nabla f_i(\mathbf{w}_{t-1})\|^2 - \|\nabla F(\mathbf{w}_{t-1})\|^2 - \|\nabla f_i(\mathbf{w}_{t-1})\|^2\} \quad (15b)$$

$$= \frac{\eta}{2} \sum_{i \in \mathcal{I}} \gamma_t^i x_t^i [\mathbb{E}\{\|\nabla F(\mathbf{w}_{t-1}) - \nabla f_i(\mathbf{w}_{t-1})\|^2\} - \mathbb{E}\{\|\nabla F(\mathbf{w}_{t-1})\|^2\} - \mathbb{E}\{\|\nabla f_i(\mathbf{w}_{t-1})\|^2\}] \quad (15c)$$

where (15a) holds because  $\langle \mathbf{a} + \mathbf{b}, \mathbf{c} \rangle = \langle \mathbf{a}, \mathbf{c} \rangle + \langle \mathbf{b}, \mathbf{c} \rangle$  and  $\langle m\mathbf{a}, \mathbf{b} \rangle = m\langle \mathbf{a}, \mathbf{b} \rangle$  for any  $\mathbf{a}, \mathbf{b}$ , and  $\mathbf{c}$ . Here (15b) holds because  $\langle \mathbf{a}, \mathbf{b} \rangle = \frac{1}{2}(\|\mathbf{a}\|^2 + \|\mathbf{b}\|^2 - \|\mathbf{a} - \mathbf{b}\|^2)$ . Finally, (15c) is a trivial decomposition of expectation on additive terms.

Putting (14) and (15) back into (13), sorting the terms a bit, and utilizing bounded divergences of global and local empirical risk functions, the theorem then follows.  $\square$

## B. Solution Scheme and Algorithm Design

For  $U(F(\mathbf{w}_t))$  in (12),  $-\frac{\eta}{2} \sum_{i \in \mathcal{I}} x_t^i \gamma_t^i \mathbb{E}\{\|\nabla F(\mathbf{w}_{t-1})\|^2\}$  is non-linear in  $\mathbf{x}$  according to (10), and calculating this term requires uploading the local gradients (hence a large amount of data), rather than the gradients' norm. We omit this term for linearity and tractability while maintaining the property of upper bound, as this term is negative. Since  $\mathbb{E}\{F(\mathbf{w}_{t-1})\}$  is not related to client selection  $\mathbf{x}_t$ , solving (11) becomes:

$$\min_{\substack{\theta, \mathbf{x}, \mathbf{y}, \mathbf{z} \\ 0 \leq \phi^\downarrow, \phi^\uparrow \leq c}} \sum_{i \in \mathcal{I}} x_t^i \gamma_t^i \{(LCI\eta\gamma_t^i - 1) \mathbb{E}\{\|\nabla f_i(\mathbf{w}_{t-1})\|^2\} + \epsilon^2\} \quad (16a)$$

s.t. (1), (2), (5) – (9)

$\theta, \mathbf{x}, \mathbf{y}, \mathbf{z} \in \text{binary}, \phi^\downarrow \in \text{integer}, \phi^\uparrow \in \text{continuous}$

Note that  $\epsilon^2$  is an empirical constant, and  $\|\nabla f_i(\mathbf{w}_{t-1})\|^2$  and  $\gamma_t^i$  are posterior after local training. Hence problem (16) is naturally decomposed into two sub-problems. In the first stage, we optimize the candidate set of clients and routing for downloading ( $\theta, \mathbf{y}$ , and  $\phi^\downarrow$ ). In the second stage, with the reported information of  $\|\nabla f_i(\mathbf{w}_{t-1})\|^2$  and  $\gamma_t^i$  from the each candidate client  $i$ , we optimize the client selection and routing for uploading ( $\mathbf{x}, \mathbf{z}$ , and  $\phi^\uparrow$ ).

For the first stage, the proposed algorithm is given in Algorithm 1. Line 1 determines  $\theta_t$ , where  $\mathcal{I}'_t \subseteq \mathcal{I}$  is the set of the available satellites in round  $t$ , depending on their local energy supply and real-time load (see Footnote 3). In Line 1,  $\beta$  is used to control the scale of the candidate set, with a trade-off between the time cost (of downloading the global model and local training) and the probability of getting significant parameter updates. Using distribution  $\gamma_t$  results in preference on satellites with larger local datasets [7], while maintaining the randomness of sampling. For the routing optimization, we aim at minimizing a weighted sum of the end time of downloading the global model to the candidate satellites:

$$\min_{\mathbf{y}_t, 0 \leq \phi_t^\downarrow \leq c, \phi_t^\downarrow \in \text{integer}} \sum_{i \in \mathcal{I}} \sum_{k \in \mathcal{K}_t} k \mu_t^i y_t^{ik}, \text{ s.t. (5) and (6)} \quad (17)$$

where  $\mu_t^i = H_t^i / h_t^{K_t}$  gives more importance to the satellites that require longer time on local training. Recall that the solution of  $\phi_t^\downarrow$  should be integral. Nevertheless, in Lines 2 to 9 of Algorithm 1, we derive an optimal algorithm based on a modified time-varying graph (denoted by  $G'$ ) and LP relaxation. In  $G'$ , an additional sink node is denoted by  $d$  and the unit flow cost of each arc  $(u, v)$  is denoted by  $q^{(u, v)}$ .

**Lemma 2.** *The linear program (LP) in Line 7 of Algorithm 1 has integer property.*

*Proof.* From its structure, this LP describes a minimum cost flow problem with a totally unimodular coefficient matrix, integer arc capacity and right-hand side of constraints. Thus, the optimal  $\phi_t^\downarrow$  is integer [15].  $\square$

**Theorem 3.** *Lines 2 to 9 of Algorithm 1 are of polynomial-time complexity and solve the problem in (17) to optimum.*

*Proof.* The LP in Line 7 is solvable in polynomial time, and the other calculations are polynomial-time as well. Note that this LP has an objective function that is equivalent to that of (17). Due to Lemma 2, the feasible solutions of this LP and (17) are in one-to-one mapping. The mapping from the former to the latter is via letting  $i \setminus \kappa$  be a sink node with demand one and setting  $\phi_t^{\downarrow(i \setminus \kappa, d)} = 0$  for  $i \in \mathcal{I}$  with  $y_t^{i \setminus \kappa} = 1$ , and keeping the rest of the flow solution. Vice versa for the mapping of the other direction. Hence the conclusion.  $\square$

---

**Algorithm 1** Candidate Decision and Routing Algorithm

---

- 1:  $\theta_t \leftarrow$  Randomly select  $\min\{(1 + \beta)CI, |\mathcal{I}_t|\}$  satellites from  $\mathcal{I}'_t$ , with probability distribution  $\gamma_t$
- 2:  $G'_t = (V'_t, E'_t) \leftarrow G_t$  with  $q^{(u,v)} = 0 \forall (u, v) \in E_t$
- 3: **for**  $k \in \{1, 2, \dots, K_t\}$  **do**
- 4:     **for**  $i \in \mathcal{I}$  with  $\theta_t^i = 1$  **do**
- 5:         Add arc  $(i \setminus k, d)$  to  $G'_t$ , with  $q^{(i \setminus k, d)} = k\mu_t^i$  and  $c^{(i \setminus k, d)} = 1$
- 6: Relax  $\phi_t^{\downarrow}$  to be continuous variables
- 7: Solve LP  $\min_{0 \leq \phi_t^{\downarrow} \leq c} \sum_{(u,v) \in E'_t} q^{(u,v)} \phi_t^{\downarrow(u,v)}$

$$\text{s.t. } \sum_{(u,v) \in E'_t} \phi_t^{\downarrow(u,v)} - \sum_{(v,u) \in E'_t} \phi_t^{\downarrow(v,u)} = \begin{cases} CI, & u = s \setminus 0 \\ -CI, & u = d \\ 0, & \text{otherwise} \end{cases}$$

- 8: **for**  $i \in \mathcal{I}$  with  $\theta_t^i = 1$  **do**
  - 9:      $y_t^{i \setminus \kappa} \leftarrow 1$  where  $\kappa = \max\{k \in \mathcal{K} | \phi_t^{\downarrow(i \setminus k, d)} > 0\}$
- 

The information of  $\|\nabla f_i(\mathbf{w}_{t-1})\|^2$  and  $\gamma_t^i$  is then returned to the server from each candidate client  $i$ . In the second stage, the optimization reduces to:

$$\min_{\mathbf{x}, \mathbf{z}, \phi^{\uparrow}} \sum_{i \in \mathcal{I}} x_t^i \gamma_t^i \left\{ (LCI\eta\gamma_t^i - 1) \mathbb{E}\{\|\nabla f_i(\mathbf{w}_{t-1})\|^2\} + \epsilon^2 \right\} \quad (18a)$$

s.t. (1), (2), (7) – (9).

**Theorem 4.** *The problem in (18) is NP-hard.*

*Proof.* We make a reduction from the minimum vertex cover (MVC) problem of any graph  $G^* = (V^*, E^*)$  to our problem. Obviously, one can solve MVC if one can answer the following question: For each number  $n$  ranging from 1 to  $|V^*|$ , can all edges be covered by selecting  $n$  nodes?

We construct a special case of (18) with graph  $G$  for a single snapshot as follows: 1) There is a node for each node  $u$  in  $V^*$ , representing a candidate client, with demand  $|E^*|$  and utility one, 2) there is a node for each arc  $(u, v)$  in  $E^*$ , 3) there is a sink node  $s$ , representing the server, and 4) there is an auxiliary node  $a$ . There are arcs of four types in  $G$ , for all  $u, v \in V^*$  and  $(u, v) \in E^*$ : 1) from nodes  $u$  and  $v$  to node  $(u, v)$  with capacity  $M \gg |E^*|$ , 2) from node  $(u, v)$  to node  $s$  with capacity one, 3) from node  $u$  to node  $a$  with capacity  $|E^*|$ , and 4) from node  $a$  to node  $s$  with capacity  $(n-1)|E^*|$ . One can show that whether or not it is feasible to select  $n$  clients, with the total flow of  $n|E^*|$ , gives the correct answer to the MVC problem. Hence the theorem follows.  $\square$

The mixed integer linear programming (MILP) problem in (18) can be solved to optimum via an off-the-shelf solver. We also propose a faster heuristic algorithm: Constraints (1) and (9) are dealt with by pre-processing, as  $\theta$  and  $\mathbf{y}$  are known. Next, the candidate satellites are sorted according to their coefficients in (18a) in descending order, and then selected greedily in turn with routing feasibility check. If adding a client causes infeasibility, it is permanently skipped. The feasibility is checked by the following: Construct  $G'_t = (V'_t, E'_t) \leftarrow G_t$  with  $q^{(u,v)} = 0, (u, v) \in E_t$ . For each satellite  $i$  with  $x_t^i = 1$ , add arcs  $(i \setminus \kappa(i), s \setminus K_t)$  with  $q^{(i \setminus \kappa(i), s \setminus K_t)} = 1$  and  $c^{(i \setminus \kappa(i), s \setminus K_t)} = I$  to  $G'_t$ , and let  $z_t^{i \setminus \kappa(i)} \leftarrow 1$  where  $\kappa(i)$  is the earliest snapshot that satisfies (9). Next, solve the LP  $\min_{0 \leq \phi_t^{\uparrow} \leq c} \sum_{(u,v) \in E'_t} q^{(u,v)} \phi_t^{\uparrow(u,v)}$  s.t. (8) where  $E_t$  is replaced by  $E'_t$ . If the minimum cost equals zero, the routing is feasible.

The overall algorithm for client selection and routing is given in Algorithm 2, which is named UBNF, as it is based on the upper bound (UB) of global empirical risk and network flow (NF) approach for inter-satellite routing.

---

**Algorithm 2** UBNF: Client Selection and Routing Algorithm

---

**[Server satellite do]**

- 1: Initialize  $\mathbf{w}_0$  by its local parameters
  - 2: **for**  $t \in \mathcal{T}$  **do**
    - Stage 1: Candidate set and routing for downloading*
    - 3:  $\theta_t, \mathbf{y}_t$ , and  $\phi_t^{\downarrow} \leftarrow$  Algorithm 1
    - 4: **for**  $i \in \mathcal{I}$  with  $\theta_t^i = 1$  **do**
    - 5:     Send global model parameters  $\mathbf{w}_{t-1}$  to satellite  $i$ , with routing indicated by  $\mathbf{y}_t$  and  $\phi_t^{\downarrow}$
    - 6:     Receive gradient norm  $\|\nabla f_i(\mathbf{w}_{t-1})\|$  and training data size  $\gamma_t^i$  from satellite  $i$ , after its local training
    - Stage 2: Client selection and routing for uploading*
    - 7:  $\mathbf{x}_t, \mathbf{z}_t$ , and  $\phi_t^{\uparrow} \leftarrow$  Solve (18)
    - 8: **for**  $i \in \mathcal{I}$  with  $x_t^i = 1$  **do**
    - 9:     Receive the local gradient  $\nabla f_i(\mathbf{w}_{t-1})$  from satellite  $i$ , with routing indicated by  $\mathbf{z}_t$  and  $\phi_t^{\uparrow}$
    - Global aggregation*
    - 10:  $\mathbf{w}_t = \mathbf{w}_{t-1} - \eta \sum_{i \in \mathcal{I}} \gamma_t^i x_t^i \nabla f_i(\mathbf{w}_{t-1})$
- 

*C. Convergence Analysis*

Recall the assumptions in Section III-A. Similar to [16], we regard  $\lim_{T \rightarrow \infty} \mathbb{E}\{\frac{1}{T} \sum_{t=1}^T \|\nabla F(\mathbf{w}_{t-1})\|^2\} = \theta$  as the target property, to prove the convergence of  $\theta$ -suboptimal.

**Theorem 5.** *For the employed FL system with client selection, with the learning rate  $\eta \leq \frac{1}{LCI}$ , we have:*

$$\frac{1}{T} \sum_{t=1}^T \mathbb{E}\{\|\nabla F(\mathbf{w}_{t-1})\|^2\} \leq \frac{2[\mathbb{E}\{F(\mathbf{w}_0)\} - F_{inf}]}{\eta T A^{lb}} + \frac{1}{T A^{lb}} \sum_{t=1}^T \sum_{i \in \mathcal{I}} x_t^i \gamma_t^i \left\{ (LCI\eta\gamma_t^i - 1) \mathbb{E}\{\|\nabla f_i(\mathbf{w}_{t-1})\|^2\} + \epsilon^2 \right\}, \quad (19)$$

after  $T$  rounds of global aggregations, and

$$\lim_{T \rightarrow \infty} \frac{1}{T} \sum_{t=1}^T \mathbb{E}\{\|\nabla F(\mathbf{w}_{t-1})\|^2\} \leq \frac{I\epsilon^2}{A^{\text{lb}}}. \quad (20)$$

*Proof.* Denote by  $\text{RHS}_{(12)}$  the right-hand side of (12). By Theorem 1, we have  $\mathbb{E}\{F(\mathbf{w}_t)\} \leq \text{RHS}_{(12)}$ . Then by taking the average over time on both sides, we have:

$$\begin{aligned} \frac{1}{T} \sum_{t=1}^T \mathbb{E}\{F(\mathbf{w}_t)\} &\leq \frac{1}{T} \sum_{t=1}^T \mathbb{E}\{F(\mathbf{w}_{t-1})\} + \\ &\frac{\eta}{2T} \sum_{t=1}^T \sum_{i \in \mathcal{I}} x_t^i \gamma_t^i \left\{ (LCI\eta\gamma_t^i - 1) \mathbb{E}\{\|\nabla f_i(\mathbf{w}_{t-1})\|^2\} \right. \\ &\quad \left. + \epsilon^2 - \mathbb{E}\{\|\nabla F(\mathbf{w}_{t-1})\|^2\} \right\}. \end{aligned} \quad (21)$$

Next, by eliminating the overlapping terms in  $\frac{1}{T} \sum_{t=1}^T \mathbb{E}\{F(\mathbf{w}_t)\}$  and  $\frac{1}{T} \sum_{t=1}^T \mathbb{E}\{F(\mathbf{w}_{t-1})\}$ , using the assumption that  $F(\mathbf{w}_t)$  is lower-bounded, sorting the orders of terms and coefficients, we have:

$$\begin{aligned} \frac{1}{T} \sum_{t=1}^T \left[ \mathbb{E}\{\|\nabla F(\mathbf{w}_{t-1})\|^2\} \sum_{i \in \mathcal{I}} x_t^i \gamma_t^i \right] &\leq \frac{2[\mathbb{E}\{F(\mathbf{w}_0)\} - F_{\text{inf}}]}{\eta T} \\ &+ \frac{1}{T} \sum_{t=1}^T \sum_{i \in \mathcal{I}} x_t^i \gamma_t^i \left\{ (LCI\eta\gamma_t^i - 1) \mathbb{E}\{\|\nabla f_i(\mathbf{w}_{t-1})\|^2\} + \epsilon^2 \right\}. \end{aligned} \quad (22)$$

Recall that  $A^{\text{lb}}$  is a lower bound of  $\sum_{i \in \mathcal{I}} x_t^i \gamma_t^i$  for all  $t \in T$ . Denote by  $\text{LHS}_{(22)}$  the left-hand side of (22). We have:

$$\frac{A^{\text{lb}}}{T} \sum_{t=1}^T \mathbb{E}\{\|\nabla F(\mathbf{w}_{t-1})\|^2\} \leq \text{LHS}_{(22)} \leq \text{RHS}_{(22)} \quad (23)$$

Last, by dividing  $A^{\text{lb}}$  on both sides of (23), we have (19).

Next, since  $x_t^i \gamma_t^i \leq 1$ ,  $LCI\eta - 1 < 0$ , and  $\frac{1}{T} \sum_{t=1}^T I\epsilon^2 = I\epsilon^2$ , we have:

$$\frac{1}{T} \sum_{t=1}^T \mathbb{E}\{\|\nabla F(\mathbf{w}_{t-1})\|^2\} \leq \frac{2[\mathbb{E}\{F(\mathbf{w}_0)\} - F_{\text{inf}}]}{\eta T A^{\text{lb}}} + \frac{I\epsilon^2}{A^{\text{lb}}} \quad (24)$$

Hence we have the conclusion in (20).  $\square$

We remark that one practical insight of Theorem 5 is that under the same conditions otherwise, the larger the satellite network (i.e., larger  $I$ ), the slower the convergence. As another insight, the more samples used for local training (i.e., larger  $A_{\text{lb}}$ ), the faster the convergence.

#### IV. SIMULATION

We use the AGI STK software to simulate the Iridium constellation [4] in Fig. 3 with six planes and 11 LEO satellites on each plane ( $I = 66$ ). The scenario time span is set from 00:00:00 to 00:01:40 on March 14 2025 UTCG, evenly divided into 100 FL rounds with one minute per round. A satellite typically has stable connection with four adjacent ones, along with minute-level intermittent links if the distance is within 4200 km. Consequently, the duration

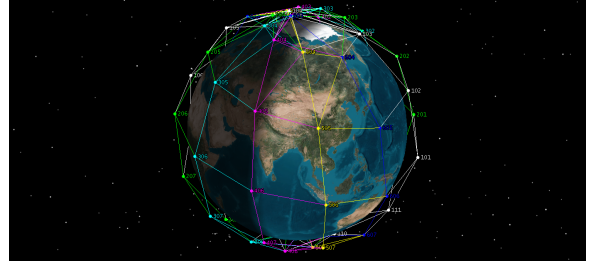


Figure 3: The Iridium constellation, where a line between two satellites means communication is available at this moment.

of a snapshot of static network topology is at second level. Microwave communication is considered, and the rates for a stable link and a intermittent link are 300 Mbps and 100 Mbps, respectively. One satellite is randomly selected as the server.

We test with dataset CIFAR-10<sup>4</sup> which consists of 10 classes of  $32 \times 32$  images. We partition the training dataset for the 66 clients under a non-independent identically distribution (non-IID) setting where the Dirichlet distribution with parameter  $\alpha \in \{0.1, 0.3\}$  is used (note that a lower value of  $\alpha$  means higher heterogeneity). The test dataset is assumed centrally hosted on the server satellite. We train a CNN model with four  $3 \times 3$  convolutional layers, two maxpool layers, and two fully connected layers, with in total 1.44 Million float-32 parameters. The model size is hence 46.08 Mbits. We adopt sampling rate  $C \in \{0.05, 0.1\}$ , scaling factor  $\beta \in \{1, 3\}$ , learning rate  $\eta = 0.1$ , minibatch size of 32, and one local epoch. The required time for local training of satellites in each round is randomly generated within 10%-60% of the duration of a round. For comparison, we consider: 1) Random client selection [1] with optimal routing. If a selected client can not finish its local training and uploading by the end of the last snapshot, this client does not join the aggregation (i.e., a timeout event), and 2) Client selection by maximizing the sum of square of gradient norm with optimal routing, named MGN-R, adapted based on the SOTA in [9], for satellite networks.

Fig. 4 shows the global model's training loss and test accuracy, under different sizes of the candidate set of our UBNF algorithm, i.e., a sensitivity analysis on  $\beta$ . UBNF greatly outperforms Random, achieving on average 10 percentage points higher test accuracy between rounds 25 to 60. Additionally, UBNF maintains a performance advantage over MGN-R before round 50. For UBNF, the performance under  $\beta = 1$  and  $\beta = 3$  stays close, though the latter is more stable with less sharp drop. It reveals that even a small candidate set (twice of the selected clients for aggregation) suffices for satisfactory performance – a valuable insight in particular for satellite networks. Fig. 5 gives the comparison under different levels of heterogeneity of non-IID training datasets. The performance of UBNF is relatively stable under different  $\alpha$ , and its advantage than Random becomes more significant

<sup>4</sup><https://www.cs.toronto.edu/~kriz/cifar.html>

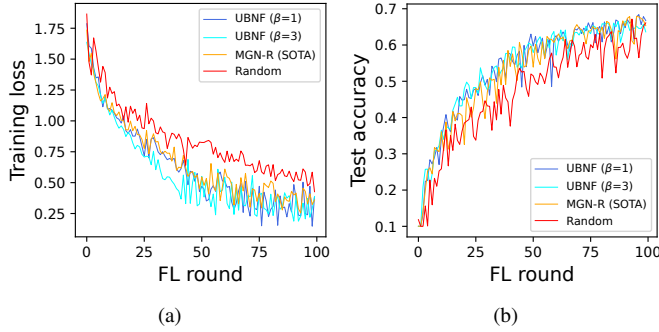


Figure 4: Training loss and test accuracy vs FL round, with  $\alpha = 0.3$ ,  $C = 0.1$ , and different candidate set sizes by  $\beta$ .

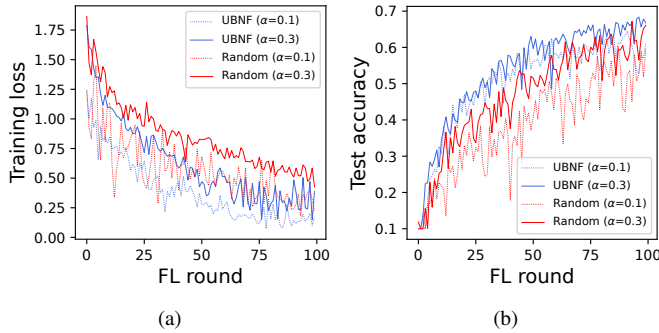


Figure 5: Training loss and test accuracy vs FL round, with  $\beta = 1$ ,  $C = 0.1$ , and different dataset heterogeneity by  $\alpha$ .

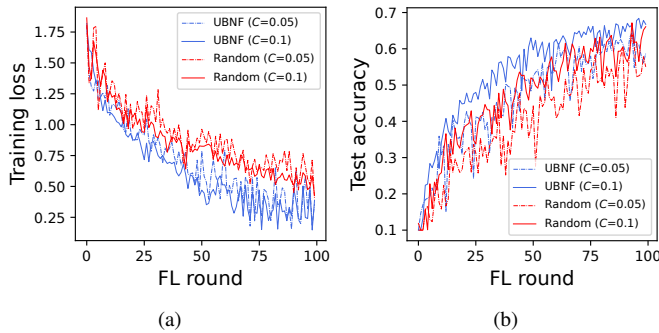


Figure 6: Training loss and test accuracy vs FL round, with  $\beta = 1$ ,  $\alpha = 0.3$ , and different sample rates by  $C$ .

under higher heterogeneity. Interestingly, both UBNF and Random achieve lower training loss yet inferior test accuracy under  $\alpha = 0.1$ , compared with  $\alpha = 0.3$ . One potential reason is overfitting under high heterogeneity to data of certain classes. Fig. 6 gives the comparison under different sample rates. For both  $C = 0.05$  and  $C = 0.1$ , UBNF significantly outperforms Random. Besides, we remark that the results of MGN-R are not shown in Figs. 5 and 6 for visual clarity, in particular as its relative performance compared with UBNF is quite similar to that in Fig. 4.

## V. CONCLUSION

We have modeled and addressed the joint optimization problem of client selection and dynamic routing for FL in satellite networks. Future work include incorporating on-orbit computing and communication resource into optimization, and simulation using satellites' remote sensing datasets.

## ACKNOWLEDGEMENTS

The research work has been partially funded by Swedish Research Council with grant number 2022-04123.

## REFERENCES

- [1] B. McMahan, E. Moore, D. Ramage, S. Hampson, and B. A. y Arcas, "Communication-efficient learning of deep networks from decentralized data," in *Artificial Intelligence and Statistics*. PMLR, 2017, pp. 1273–1282.
- [2] Y. Pan, C. Zhu, L. Luo, Y. Liu, and Z. Cheng, "FedTrack: A collaborative target tracking framework based on adaptive federated learning," *IEEE Transactions on Vehicular Technology*, vol. 73, no. 9, pp. 13 868–13 882, 2024.
- [3] C. Yang, J. Yuan, Y. Wu, Q. Sun, A. Zhou, S. Wang, and M. Xu, "Communication-efficient satellite-ground federated learning through progressive weight quantization," *IEEE Transactions on Mobile Computing*, vol. 23, no. 9, pp. 8999–9011, 2024.
- [4] H. Zhang, H. Zhao, R. Liu, X. Gao, and S. Xu, "Leader federated learning optimization using deep reinforcement learning for distributed satellite edge intelligence," *IEEE Transactions on Services Computing*, vol. 17, no. 5, pp. 2544–2557, 2024.
- [5] Z. Zhai, Q. Wu, S. Yu, R. Li, F. Zhang, and X. Chen, "FedLEO: An offloading-assisted decentralized federated learning framework for low earth orbit satellite networks," *IEEE Transactions on Mobile Computing*, vol. 23, no. 5, pp. 5260–5279, 2024.
- [6] Z. Yan and D. Li, "Convergence time optimization for decentralized federated learning with LEO satellites via number control," *IEEE Transactions on Vehicular Technology*, vol. 73, no. 3, pp. 4517–4522, 2024.
- [7] L. Fu, H. Zhang, G. Gao, M. Zhang, and X. Liu, "Client selection in federated learning: Principles, challenges, and opportunities," *IEEE Internet of Things Journal*, vol. 10, no. 24, pp. 21 811–21 819, 2023.
- [8] S. Mayhoub and T. M. Shami, "A review of client selection methods in federated learning," *Archives of Computational Methods in Engineering*, vol. 31, no. 2, pp. 1129–1152, 2024.
- [9] O. Marnissi, H. E. Hammouti, and E. H. Bergou, "Client selection in federated learning based on gradients importance," in *AIP Conference Proceedings*, vol. 3034, no. 1. AIP Publishing, 2024.
- [10] Y. J. Cho, J. Wang, and G. Joshi, "Client selection in federated learning: Convergence analysis and power-of-choice selection strategies," *arXiv preprint arXiv:2010.01243*, 2020.
- [11] C. Feng, Y. Wang, Z. Zhao, T. Q. S. Quek, and M. Peng, "Joint optimization of data sampling and user selection for federated learning in the mobile edge computing systems," in *2020 IEEE International Conference on Communications Workshops*, 2020, pp. 1–6.
- [12] T. Zhang, J. Li, H. Li, S. Zhang, P. Wang, and H. Shen, "Application of time-varying graph theory over the space information networks," *IEEE Network*, vol. 34, no. 2, pp. 179–185, 2020.
- [13] Z. Tang, Z. Feng, W. Han, W. Yu, B. Zhao, and C. Wu, "Improving the snapshot routing performance through reassigning the inter-satellite links," in *2015 IEEE Conference on Computer Communications Workshops (INFOCOM WKSHPS)*, 2015, pp. 97–98.
- [14] Z. Han, C. Xu, G. Zhao, S. Wang, K. Cheng, and S. Yu, "Time-varying topology model for dynamic routing in LEO satellite constellation networks," *IEEE Transactions on Vehicular Technology*, vol. 72, no. 3, pp. 3440–3454, 2023.
- [15] R. K. Ahuja, T. L. Magnanti, and J. B. Orlin, *Network flows: theory, algorithms, and applications*. USA: Prentice-Hall, Inc., 1993.
- [16] C. Feng, H. H. Yang, D. Hu, Z. Zhao, T. Q. S. Quek, and G. Min, "Mobility-aware cluster federated learning in hierarchical wireless networks," *IEEE Transactions on Wireless Communications*, vol. 21, no. 10, pp. 8441–8458, 2022.